doi:10.1093/brain/awq017 Brain 2010: 133; 690–700 | 690

BRAIN
A JOURNAL OF NEUROLOGY

Increased sensorimotor network activity in *DYT1* dystonia: a functional imaging study

Maren Carbon,[1,2] Miklos Argyelan,[1] Christian Habeck,[3] M. Felice Ghilardi,[4] Toni Fitzpatrick,[1] Vijay Dhawan,[1,2] Michael Pourfar,[1,2] Susan B. Bressman[5] and David Eidelberg[1,2]

1 Centre for Neurosciences, The Feinstein Institute for Medical Research, Manhasset, NY, USA
2 Departments of Neurology and Medicine, North Shore University Hospital and New York University School of Medicine, New York, NY, USA
3 Cognitive Neuroscience Division, Taub Institute, Columbia University Medical Centre, New York, NY, USA
4 Department of Pharmacology and Physiology, CUNY Medical School at City College of New York, New York, NY, USA
5 Mirken Department of Neurology, Beth Israel Medical Centre, New York, NY, USA

Correspondence to: Dr Maren Carbon, MD,
Centre for Neurosciences,
The Feinstein Institute for Medical Research,
350 Community Drive,
Manhasset,
New York 11030, USA
E-mail: mcarbon@nshs.edu

Neurophysiological studies have provided evidence of primary motor cortex hyperexcitability in primary dystonia, but several functional imaging studies suggest otherwise. To address this issue, we measured sensorimotor activation at both the regional and network levels in carriers of the *DYT1* dystonia mutation and in control subjects. We used ^{15}Oxygen-labelled water and positron emission tomography to scan nine manifesting *DYT1* carriers, 10 non-manifesting *DYT1* carriers and 12 age-matched controls while they performed a kinematically controlled motor task; they were also scanned in a non-motor audio-visual control condition. Within- and between-group contrasts were analysed with statistical parametric mapping. For network analysis, we first identified a normal motor-related activation pattern in a set of 39 motor and audio-visual scans acquired in an independent cohort of 18 healthy volunteer subjects. The expression of this pattern was prospectively quantified in the motor and control scans acquired in each of the gene carriers and controls. Network values for the three groups were compared with ANOVA and *post hoc* contrasts. Voxel-wise comparison of *DYT1* carriers and controls revealed abnormally increased motor activation responses in the former group ($P<0.05$, corrected; statistical parametric mapping), localized to the sensorimotor cortex, dorsal premotor cortex, supplementary motor area and the inferior parietal cortex. Network analysis of the normative derivation cohort revealed a significant normal motor-related activation pattern topography ($P<0.0001$) characterized by covarying neural activity in the sensorimotor cortex, dorsal premotor cortex, supplementary motor area and cerebellum. In the study cohort, normal motor-related activation pattern expression measured during movement was abnormally elevated in the manifesting gene carriers ($P<0.001$) but not in their non-manifesting counterparts. In contrast, in the non-motor control condition, abnormal increases in network activity were present in both groups of gene carriers ($P<0.001$). In this condition, normal motor-related activation pattern expression in non-manifesting carriers was greater than in controls, but lower than in affected carriers. In the latter group, measures of normal motor-related activation pattern expression in the audio-visual condition correlated with independent dystonia clinical ratings ($r=0.70$, $P=0.04$). These findings confirm that overexcitability of the sensorimotor system is a robust feature of dystonia. The presence of elevated normal motor-related activation pattern expression in the non-motor condition suggests that abnormal integration of audio-visual input with sensorimotor network activity is an

Received July 17, 2009. Revised December 22, 2009. Accepted January 11, 2010

important trait feature of this disorder. Lastly, quantification of normal motor-related activation pattern expression in individual cases may have utility as an objective descriptor of therapeutic response in trials of new treatments for dystonia and related disorders.

Keywords: *DYT1* dystonia; imaging marker; positron emission tomography; motor activation

Abbreviations: AV = audio-visual reference task; BA = Brodmann area; BFMDRS = Burke-Fahn-Marsden Dystonia Rating Scale; CCW = counterclockwise reaching motor task; OrT/CVA = ordinal trends canonical variate analysis; rCBF = regional cerebral blood flow; SPM = statistical parametric mapping

Introduction

Dystonia is a neurological syndrome manifested clinically by focal or generalized sustained muscle contractions, postures and/or involuntary movements, ranging from action-induced dystonic symptoms to disabling, generalized dystonia. The most frequent genetic form of primary torsion dystonia relates to the autosomal dominant *DYT1* mutation on chromosome 9q34, representing a GAG deletion within the coding area for torsinA (de Carvalho Aguiar and Ozelius, 2002). The link between the presence of dystonia mutations and clinical manifestations of disease is not well understood.

Abnormalities of the sensorimotor system in dystonia have been described at multiple levels (e.g. Berardelli *et al.*, 1998; Quartarone *et al.*, 2006). An overarching concept emerges from studies of focal dystonia relating the disorder to increased cortical excitability, decreased cortical inhibition, maladaptive cortical plasticity and impaired sensorimotor integration (Quartarone *et al.*, 2006). Increased cortical excitability has been shown in hereditary dystonia, regardless of clinical penetrance (Edwards *et al.*, 2003), in unaffected body parts of focal dystonia patients (Sommer *et al.*, 2002), and in relatives of patients with sporadic dystonia (Walsh *et al.*, 2007). Overall, these studies suggest that this feature represents a trait characteristic of dystonia. These observations were obtained in neurophysiological studies conducted in the resting state or during the performance of simple motor paradigms, such as flexion and extension at single joints. In this regard, functional imaging has extended these findings by delineating corresponding metabolic abnormalities at rest or abnormalities of regional brain activation during the execution of simple movements. For instance, trait characteristics have been demonstrated in a variety of imaging investigations of *DYT1* mutation carriers. Metabolic abnormalities of the basal ganglia, supplementary motor area and cerebellum are evident in *DYT1* mutation carriers scanned in the rest state (Eidelberg *et al.*, 1998; Trošt *et al.*, 2002; Carbon *et al.*, 2004*a*; see e.g. Carbon and Eidelberg, 2009 for review). Microstructural studies with magnetic resonance diffusion tensor imaging suggest that these functional changes relate to an underlying maldevelopment of cerebellar outflow pathways in mutation carriers (Carbon *et al.*, 2008*b*; *cf.* Argyelan *et al.*, 2009). Indeed, we have found increased activation of secondary motor regions and inferior parietal cortex in non-manifesting *DYT1* carriers, accompanied by reduced activation of the right inferior cerebellum (Ghilardi *et al.*, 2003).

In contrast to these studies in genetically homogenous populations, functional imaging of motor activation responses in sporadic dystonia has yielded inconsistent findings. Although many of these studies reported activation abnormalities within the sensorimotor system, no consistent regional pattern emerged. Despite neurophysiological evidence of disinhibited sensorimotor cortex activity in dystonia, abnormally increased sensorimotor cortex activation has been demonstrated in some studies (Odergren *et al.*, 1998; Pujol *et al.*, 2000; Preibisch *et al.*, 2001; Blood *et al.*, 2004; Lerner *et al.*, 2004; Hu *et al.*, 2006), while decreased activation in this region was reported in others (Ceballos-Baumann *et al.*, 1995*b*; Ibanez *et al.*, 1999; Oga *et al.*, 2002; Haslinger *et al.*, 2005; Dresel *et al.*, 2006). Similar discrepancies exist regarding activation changes in secondary motor regions. Moreover, to date, few imaging studies have examined the functional changes occurring in dystonia at a systems level (e.g. Ibanez *et al.*, 1999; Carbon *et al.*, 2004*b*).

In the current study, we used a new multivariate network-modelling approach for activation (Habeck *et al.*, 2005; Moeller and Habeck, 2006) to quantify the activity of the sensorimotor system as a whole in dystonia mutation carriers and in control subjects. In addition to clinically affected subjects, we studied non-manifesting mutation carriers in order to distinguish intrinsic genotypic abnormalities from symptom-related changes. A combined behavioural and neuroimaging approach was used to: (i) identify abnormal movement characteristics during the performance of a repetitive reaching task in *DYT1* carriers; (ii) identify abnormal motor activation responses in *DYT1* carriers; and (iii) quantify sensorimotor network activity in *DYT1* carriers and controls in ^{15}O-labelled water ($H_2^{15}O$) PET scans acquired during movement and in a controlled audio-visual state without movement.

Materials and methods

This study was divided into three parts: (i) a behavioural study of repetitive reaching movements; (ii) a univariate voxel-wise analysis of regional cerebral blood flow (rCBF) measured during repetitive reaching movements and in a non-motor audio-visual control condition; and (iii) a multivariate spatial covariance analysis of the rCBF data to quantify sensorimotor network activity in the same conditions.

Subjects

The following groups of right-handed subjects were included.

(i) *DYT1* mutation carriers: 11 clinically manifesting mutation carriers [42.8 ± 15.5 years (mean ± SD)] and 10

non-manifesting mutation carriers (age 51.5 ± 14.3 years; manifesting versus non-manifesting comparison $P > 0.2$, Student's *t*-test). Two of the manifesting subjects chose to participate in the behavioural testing, but not in the PET studies. Thus, a total of nine affected carriers (age 46.1.8 ± 15.1 years; manifesting versus non-manifesting comparison $P > 0.4$, Student's *t*-test) participated in the imaging experiments in addition to the behavioural studies.

(ii) Healthy controls: 12 healthy control subjects (age 44.7 ± 12.7 years; $P > 0.3$, Student's *t*-tests, for age comparison with manifesting and non-manifesting *DYT1* carriers) served as controls for both the behavioural and imaging experiments.

The *DYT1* mutation carriers were recruited and genetically tested through the Neurology Department at Beth Israel Medical Centre in New York. The control cohort consisted of patient spouses and healthy volunteers from the community. Given the very low prevalence of *DYT1* mutation in the general population, the likelihood that any one of these healthy subjects was a carrier was negligible (0.1%) (Ghilardi *et al.*, 2003). Data on the genotype-specific aspects of brain activation in a subgroup of the non-manifesting *DYT1* cohort have appeared previously (Ghilardi *et al.*, 2003). (Elements of these previously published non-manifesting *DYT1* activation data were included in this study to compare with corresponding data from the manifesting *DYT1* carriers. Genotype-related effects in non-manifesting *DYT1* carriers were reported in detail in the earlier publication.)

The clinical characteristics of the affected subjects are provided in Table 1. Exclusion criteria for all subjects were: (i) past history of additional neurological illness; (ii) prior or current exposure to neuroleptic agents or drug use; (iii) past medical history of hypertension, cardiovascular disease or diabetes mellitus; and (iv) abnormal MRI. For controls and non-manifesting subjects, the following additional exclusion criteria were applied: (i) current use of psychotropic medication; (ii) abnormal neurological examination; and (iii) past history of dystonic symptoms.

Tasks

All subjects performed a simple motor execution task involving repetitive counterclockwise reaching movements (CCW) and an audio-visual (AV) control task involving AV perception of the target display without movement (Ghilardi *et al.*, 2003). These two tasks were performed in a pseudo-random order over subjects to counter time and order effects. All subjects were trained to perform the motor task outside the scanner 1–7 days prior to the imaging session. For CCW, subjects moved a cursor on a digitizing tablet with their right hand out and back from a central starting point to one of eight radially arrayed targets. Subjects were instructed to make movements with sharp reversal inside each target. Targets appeared on a computer screen in synchrony with a tone at a constant interval of 1–2 s. The default tone interval was 1 s and was determined during the training session. The interval was lengthened only if the subject could not correctly reach >60% of the targets within the time frame. The individual paces of the movements are provided in Table 1. The movement extent was kept constant across all individuals and measurements. During the AV condition (analogous to the S task employed in previous studies, Ghilardi *et al.*, 2000), subjects remained immobile but experienced comparable AV stimuli as during the activation task. Screen targets, cursor images and tones were presented to the subjects asynchronously and irregularly in equal numbers to those used in the motor task. Although in the AV condition, subjects merely observed the screen and no movement was required during the imaging sessions, the rate of target appearance was matched to the rate used for CCW during imaging sessions.

Performance measures

To quantify motor performance during CCW, tangential velocities and accelerations were computed from hand position data. Automatic routines were used to identify the time and position at movement onsets, peak velocities, peak accelerations and reversals. Cursor positions at direction reversals were taken as the aimed end points for each movement; those at zero, calculated backwards from peak velocities, define onsets.

Table 1 Clinical characteristics of the manifesting *DYT1* mutation carriers

Subject	Age (years)	Symptom duration (years)	Distribution (body part)[a]	BFMDRS motor score	Medications[b]	CCW pace, Hz
1	23	13	Generalized (Lg, rA)	17	THX, baclofen	1
2	24	11	Focal (rA)	1	THX	1
3	40	31	Generalized (A, Lg, T)	33	THX, baclofen, zonisamide	1
4[c]	24	14	Generalized (C, A, Lg, T)	68	Ethopropazine, baclofen	2
5[c]	31	15	Focal (rA)	4	None	1
6	41	32	Generalized (C, A, Lg, T)	54	THX	1
7	43	36	Generalized (C, A, Lg, T)	17	THX, levodopa, zonisamide	1
8	57	50	Generalized (C, rA, rLg)	23	Topiramate	1.16
9	57	45	Generalized (C, rA, Lg)	6.5	Levodopa	1.3
10	64	54	Generalized (C, A, Lg, T)	35	THX	2
11	65	57	Multifocal (A, Lg)	19	None	1
Median	**41**	**32**		**19**		**1**

a r = right; Lg = leg; A = arm; T = trunk; C = craniofacial.
b THX = trihexphenidyl.
c Motor testing only, no imaging.

The following spatial and temporal characteristics were quantified for all movements: (i) movement time (the time from movement onset to the end point); (ii) spatial error (the shortest distance of the end point of the movement trajectory from the centre of the target, which the movement trajectory targeted); and (iii) onset time (the time from target and tone presentation to movement onset). Negative values indicate responses that are initiated before the tone, as required in this task.

All movements in which targets were reached within a time window of 250 ms prior to and after each tone were classified as correct. The percentage of correct movements was considered as a global measure of motor performance. Movement time, spatial error and onset time were calculated for all correct movements and used as analytical performance measures. We also computed a variability measure for movement time defined as its standard deviation (SD) over each 90 s trial.

Imaging studies

Subjects

Nineteen *DYT1* carriers (9 manifesting *DYT1*, age 46.1.8 ± 15.1 years; 10 non-manifesting *DYT1*, 51.5 ± 14.3 years, manifesting versus non-manifesting comparison $P > 0.4$, Student's *t*-test) performed the CCW and AV tasks while undergoing $H_2^{15}O$ PET imaging. Scans from 12 healthy volunteers were used as controls for the motor activation imaging experiments (age 44.7 ± 12.7 years; comparisons with either group of *DYT1* carriers $P > 0.3$, Student's *t*-tests). To identify a spatial covariance pattern corresponding to the normal motor activation network, we utilized a separate set of scans acquired in 18 different healthy volunteer subjects (age 37.2 ± 13.4 years). Each of these normal subjects performed 2–3 task repetitions during PET scanning, yielding a total of 78 scans (39 CCW scans, 39 AV scans) for pattern derivation (see below).

All $H_2^{15}O$ PET scans were performed using the GE Advance tomograph at North Shore University Hospital as described in detail elsewhere (Carbon *et al.*, 2008*a*). Motor tasks were performed with the dominant right hand, an intravenous catheter for $H_2^{15}O$ delivery was placed in the non-dominant left hand. For each task run, relative rCBF was estimated using a slow bolus method in which 10 mCi of $H_2^{15}O$ (Ferrieri *et al.*, 1994) in 4 ml saline was injected by automatic pump over 16 s (15 ml/min) followed by a manual 3 ml saline flush. $H_2^{15}O$ was produced remotely and delivered by the automatic pump (Nakamura *et al.*, 2001). Dynamic 3D PET data acquisition began at the time of radioactivity arrival in the brain and continued for 80 s thereafter. Reconstructed PET images were corrected for random coincidences, electronic dead time and tissue attenuation by transmission scans. A single scalar correction was used to compensate for scatter effects.

Each subject was scanned while performing the CCW and AV tasks in randomized order with the dominant right arm. Each task was repeated 2–3 times per subject. Digital recordings of the hand position were acquired for every run during the motor task. For the manifesting *DYT1* carriers, anti-dystonic and psychotropic medications were discontinued for at least 12 h before imaging. These subjects were also rated according to the Burke-Fahn-Marsden Dystonia Rating Scale (BFMDRS) at the time of imaging. Ethical permission for these studies was obtained from the Institutional Review Board of North Shore University Hospital. Written consent was obtained from each subject following detailed explanation of the procedures.

Univariate analysis: statistical parametric mapping

Imaging data processing was performed using statistical parametric mapping (SPM)-5 software (Institute of Neurology, London, UK; http://www.fil.ion.ucl.ac.uk/spm/software/spm5/). Standard pre-processing (realignment, spatial normalizing, smoothing with 10 _ 10 _ 10 mm) was applied followed by univariate and multivariate analyses.

Voxel-wise comparisons were performed using the flexible factorial model implemented in SPM5. We controlled for the effect of potential global blood flow differences by a global normalization to 50 ml/min/dl. SPM{*t*} maps were generated to assess the effects of task (AV, CCW) and group (control, non-manifesting *DYT1*, manifesting *DYT1*), and the interaction of these factors. To control for potential confounds resulting from the variability in task pace, the intertone interval was entered as a covariate of no interest. Contrasts were defined according to the specific questions. In particular, searches for abnormal motor activation responses in manifesting *DYT1* were performed in the flexible factorial model (i) as contrasts of task-specific activation [manifesting *DYT1* (CCW–AV) versus control (CCW–AV)]; and (ii) as within-condition contrasts between groups. In addition to searching for within-condition group effects in the CCW condition, we also explored group effects in the AV condition. To optimize the power of our inference, we restricted our search volume to areas showing a significant main effect of motor activation (CCW > AV). Crucially, this contrast is orthogonal to the simple main effect of group within the AV conditions and cannot bias our inference. For all voxel-based analyses, results were considered significant at $P < 0.05$ (false discovery rate corrected) (Genovese *et al.*, 2002), with a cluster extent cut-off of $[k_e] > 80$ voxels. Coordinates were reported in the standard anatomical space developed at the Montreal Neurological Institute.

To assess the effects of genotype in the clusters that differed in manifesting *DYT1* and controls, we extended the results of the voxel-based searches by incorporating a *post hoc* volume-of-interest analysis. To address the possibility that non-manifesting *DYT1* takes an intermediate position between manifesting and controls, volume-of-interest analysis was applied to all the significant clusters identified in the voxel-based comparisons of manifesting *DYT1* and controls. To do this, we averaged data within spherical volumes-of-interest (10 mm diameter) centred on the maxima and submaxima of the statistical parametric mapping clusters detected in the manifesting *DYT1* and control contrasts. These measures were compared using ANOVA, followed by Tukey–Kramer honestly significant difference for pairwise group comparisons (controls, non-manifesting *DYT1*, manifesting *DYT1*). The resulting activations were also depicted graphically.

Multivariate analysis: ordinal trends

In addition to univariate assessments of between-group differences in regional activation, we employed a multivariate approach to examine group differences at the network level. Specifically, we sought to determine whether the activity of the normal sensorimotor network is elevated in dystonia mutation carriers, and whether this increase is greater in manifesting relative to non-manifesting gene-positive subjects. To test this hypothesis, we first identified and validated a significant activation pattern in healthy subjects. This spatial covariance pattern was derived using $H_2^{15}O$ PET scans from a group of healthy subjects that was independent of those used as controls for comparison with the gene carriers (see above).

The procedure used to identify this pattern was based on ordinal trends canonical variate analysis (OrT/CVA) (Habeck *et al.*, 2005). OrT/CVA is a supervised principal component analysis designed to

identify spatial covariance patterns that change in expression within subject across experimental conditions. The property of consistent change in pattern expression across tasks/conditions is called an 'ordinal trend'. This attribute differs from routine assessments of task-related changes at the group mean level, employing mass univariate procedures such as statistical parametric mapping (Moeller and Habeck, 2006). In addition to detecting one or more significant activation patterns, OrT/CVA quantifies the expression of the resulting pattern(s) in each subject and condition. The significance of OrT/CVA patterns is assessed by permutation testing of the relevant subject scores to exclude the possibility that the observed changes across conditions had occurred by chance. Likewise, the reliability of the regional contributions to the pattern (i.e. the voxel weights) is assessed by bootstrap estimation (Efron and Tibshirani, 1994). The test–retest reliability of the subject scores measured in each condition is assessed across repeat runs conducted within the imaging session. Once validated, pattern expression can be quantified on a prospective case basis in scans obtained in new subject cohorts.

In this study, OrT/CVA was applied to 39 pairs of CCW and AV scans (a total of 78 $H_2^{15}O$ PET images from the independent normal cohort of 18 subjects described above). This analysis was used to identify significant and stable normal motor-related activation pattern topography. The expression of this pattern was then quantified prospectively in the scans of the *DYT1* carriers and in the second group of healthy controls that was age-matched to the gene-positive subjects. Thus, these computations were performed on an individual case basis in each of the scans (CCW and AV) separately acquired in the manifesting *DYT1*, non-manifesting *DYT1* and control subjects. For each experimental condition, between-group differences were assessed using ANOVA followed by *post hoc* tests (Tukey's honestly significant difference for data with equal variance and Dunnett's T3 test for data with unequal variance). For the manifesting *DYT1* group, we correlated pattern expression in each condition with BFMDRS motor ratings acquired at the time of PET. Correlations were assessed using Spearman rank correlation coefficients. JMP (SAS Institute Inc., Cary, NC, USA) or the Statistical Package for the Social Sciences (SPSS, Inc., Chicago, IL, USA) were used for statistical analyses. All results were considered significant for $P<0.05$.

Results

Behavioural findings

General motor task performance, expressed as the percentage of correctly hit targets, was reduced in manifesting *DYT1* ($49.4 \pm 11.4\%$, mean $\pm$ SD) compared to controls as well as to their non-manifesting counterparts (controls: $85.1 \pm 7.2\%$; non-manifesting *DYT1*: 77.4 ± 4.8; $P=0.004$, Supplementary Table S1). For the correct movements, there was a significant group difference in movement time variability (SD). This measure was higher in manifesting *DYT1* relative to age-matched controls and non-manifesting *DYT1* carriers (movement time_SD: manifesting: 103.6 ± 9.0 ms; controls: 60.5 ± 12.0 ms; non-manifesting *DYT1*: 69.7 ± 11.3; $P=0.003$). This indicates greater irregularity of the repetitive reaching movements in the affected carriers. The remaining temporal and spatial movement descriptors did not differ across groups ($P \geqslant 0.15$ for all comparisons). In line with our earlier results (Ghilardi *et al.*, 2003), all measures of motor task performance were normal in non-manifesting mutation carriers (Supplementary Table S1).

Imaging findings

Statistical parametric mapping

Within-group comparisons

In manifesting *DYT1*, significant motor activation responses (CCW > AV) were found in the left sensorimotor cortex (BA 1–4) extending into adjacent premotor (BA 6, dorsal premotor cortex and supplementary motor area), preparietal (BA 5), parietal (BA 40) and cingulate cortices (BA 24) (Supplementary Table S2). Significant activation responses were also detected in the left thalamus (ventral postero-lateral nucleus, ventral postero-medial nucleus), in the putamen bilaterally, and in the right superior cerebellar cortex (lobulus IV–VI), extending into the dentate nucleus, vermis and the left superior cerebellar cortex. Similar activation responses were found in both the non-manifesting *DYT1* and healthy volunteer groups (Supplementary Table S2).

Between-group comparisons

Relative to controls, manifesting *DYT1* exhibited increased motor activation (Fig. 1A–C) in the left sensorimotor cortex extending into adjacent secondary motor, preparietal and cingulate areas and into the homologous region of the right hemisphere (Panel A in Table 2). No significant decreases in motor activation responses were found in manifesting *DYT1* relative to controls. Except for those regions with abnormal increases in motor activation in manifesting *DYT1*, there were no other significant regional differences on comparison of manifesting *DYT1* to non-manifesting *DYT1*. Comparisons of motor task-specific activation between groups (Panel B in Table 2) showed an increase in the inferior parietal cortex in manifesting *DYT1*. In this region (Fig. 1D), significant deactivation (CCW < AV) was present during task performance in healthy subjects. The magnitude of this deactivation response was attenuated in non-manifesting *DYT1* carriers and failed to occur in their affected counterparts.

To address the effect of genotype on the abnormal manifesting *DYT1* activations, volume-of-interest comparisons were performed on the data from the manifesting *DYT1*, non-manifesting *DYT1* and control groups (see the 'Material and methods' section). Abnormal activation of the left sensorimotor cortex, supplementary motor area, cingulate and superior parietal regions (Panel A in Table 2) was specific for the affected carriers, and was not present in the non-manifesting carriers (Fig. 1A and B). In contrast, motor activation of the left dorsal premotor cortex was abnormally increased in *DYT1* mutation carriers irrespective of penetrance. In this region (Fig. 1C), non-manifesting *DYT1* carriers assumed an intermediate position between affected carriers and controls. Similar changes were present in the right supplementary motor area.

Analyses of the volume-of-interest data for each region confirmed that the significant group differences during motor task performance were not attributable to underlying group differences in rCBF recorded in the AV reference condition.

Significant differences were also present in group comparisons of rCBF recorded in the non-motor AV condition. In this condition,

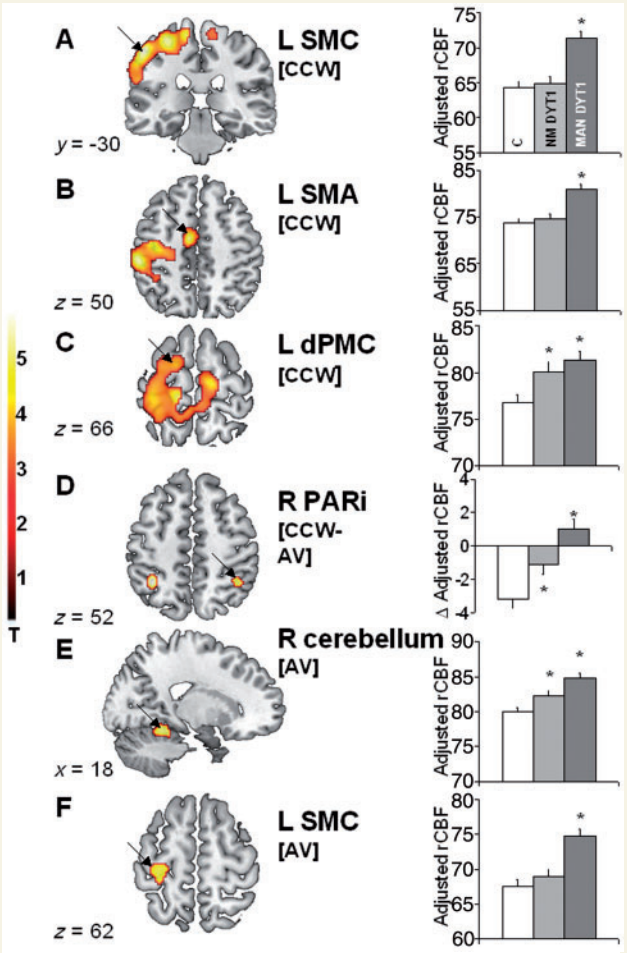

Figure 1 Brain regions with abnormal activation in manifesting *DYT1* carriers (Table 2, see text). SPM{*t*} maps (left) were superimposed on a single-subject MRI T_1 template (*x*, *y*, *z* coordinates in MNI space indicate the position of the slice). The colour scale represents *t*-values thresholded at 3.5 corresponding to $P<0.05$ false discovery rate corrected. Bar diagrams (right) of adjusted rCBF measured during performance of the motor task (CCW) or in the non-motor audio-visual control condition (AV) (see text). For each volume-of-interest, rCBF values (mean ± SE) were displayed for manifesting (MAN) *DYT1* (dark grey), non-manifesting (NM) *DYT1* (light grey), and control subjects (white). Increased motor activation was present in affected carriers in the left sensorimotor cortex (SMC, **A**), supplementary motor area (SMA, **B**), and in the dorsal premotor cortex (dPMC, **C**). Loss of task-related deactivation was evident in the inferior parietal lobule (PARi, **D**). The activation abnormalities in the sensorimotor cortex and supplementary motor area were specific for clinically affected *DYT1* carriers. In dorsal premotor cortex and PARi, abnormal activation was also present in non-manifesting gene carriers. In the non-motor AV condition, rCBF was elevated in the right cerebellum (**E**), with significant rCBF elevations in both manifesting and non-manifesting *DYT1* carriers. In contrast, in the left sensorimotor cortex (**F**), rCBF was elevated only in the affected mutation carriers. (Significant *P*-values of *post hoc* tests are denoted by asterisks).

manifesting *DYT1* carriers exhibited abnormally increased rCBF in the anterior cerebellum bilaterally and in the left sensorimotor cortex (Panel C in Table 2). In the right cerebellum (Fig. 1E), volume-of-interest analysis revealed stepwise rCBF increases in non-manifesting and manifesting *DYT1* carriers relative to controls. In contrast, in this condition, abnormally increased left sensorimotor cortex activation (Fig. 1F) was evident only in the affected carriers. Significant reductions in rCBF recorded in the AV condition were also present in the right dorso-lateral prefrontal cortex of manifesting and non-manifesting *DYT1* carriers relative to controls (Panel D in Table 2).

Ordinal trends analysis

Normal movement-related activation pattern

OrT/CVA was applied to the set of 39 cerebral blood flow scan pairs from an independent cohort of healthy subjects (age 37.2 ± 13.4 years) who performed the CCW and AV tasks (see above). An activation pattern was identified that exhibited an ordinal trend in that its expression in CCW was greater than in AV on every run ($P<0.0001$, permutation test; Fig. 2A). This normal movement-related pattern (Fig. 2B) was characterized by covarying activation of the left sensorimotor cortex (BA 1–4), premotor cortices (BA 6; dorsal premotor cortex, supplementary motor area), cingulate cortex (BA 24, 31), superior parietal (BA 5, 7), and inferior parietal (BA 40) cortices, and the occipital association region (BA 18) (Table 3). Additional regions with positive network contributions (i.e. network-related regional increases in CCW relative to AV) were identified in the left anterior cerebellar cortex, right inferior cerebellar cortex, vermis and deep cerebellar nuclei (Fig. 2A). Negative network contributions (i.e. network-related regional decreases in CCW relative to AV) were present in the right temporal (BA 21) and inferior parietal (BA 40) regions, and bilaterally in the dorsolateral prefrontal cortex (BA 46, 9) (Table 3). Voxel weights on these network regions were demonstrated to be reliable by bootstrap estimation (integrity check value extrema −5.11 to 7.85, $P<0.0001$). Subject scores on this pattern exhibited high within-session reproducibility in CCW scans (intraclass correlation coefficient 0.85, 95% CI 0.71–0.93; $P<0.0001$), and in the AV scans (intraclass correlation coefficient 0.98, 95% CI 0.95–0.99; $P<0.0001$).

Abnormal normal motor-related activation pattern expression in DYT1 carriers

Normal motor-related activation pattern expression was computed prospectively in scans from the manifesting and non-manifesting DYT1 carriers and the healthy control subjects acquired in the CCW and AV conditions. An ordinal trend across conditions (CCW > AV) was evident for each of these groups ($P<0.001$, paired *t*-tests), in that pattern expression was elevated in CCW relative to AV for each scan pair, without a single violation in the prospective control cohort and in non-manifesting *DYT1* (Supplementary Fig. S1). In manifesting *DYT1*, there were three violations in 22 scan pairs. For both conditions, significant differences in normal motor-related activation pattern expression were evident across the three groups ($P<0.001$, ANOVA; Fig. 3A). *Post hoc* testing revealed increased normal motor-related activation pattern expression in manifesting *DYT1* relative to

Table 2 Brain regions with significant differences in regional cerebral blood flow between manifesting *DYT1* carriers and controls

Voxel-based comparisons[a]: manifesting *DYT1* versus controls						Volume of interest-based comparisons[d]: manifesting *DYT1*, non-manifesting *DYT1* and controls
Brain region	Z_{max}	Coordinates (MNI)			Cluster extent	$P<0.05$
		x	*y*	*z*		
A. Manifesting *DYT1* (CCW) > controls (CCW)[b]						
L SMC (BA1–4), pre-parietal (BA5), premotor (BA6), parietal (BA7, BA40) and cingulate cortices (BA24, 31); bilateral SMA (BA6)[c]	5.4	−54	−28	52	4981	MAN > NM = C
L cingulate (submax., BA 24)[c]	5.2	−8	−8	46		MAN > NM = C
L SMA (submax., BA 6)	4.6	−12	−30	68		MAN > NM = C
R SMA (submax., BA 6)	4.5	12	−20	72		MAN > NM > C
B. Manifesting *DYT1* (CCW–AV) > controls (CCW–AV)						
L inferior parietal lobule (BA 40)[c]	5.1	−36	−48	54	128	MAN > NM = C
R inferior parietal lobule (BA 40)[c]	5.0	40	−50	46	98	MAN > NM > C
C. Manifesting *DYT1* (AV) > controls (AV)[b]						
R anterior cerebellum[c]	4.9	16	−44	−14	478	MAN > NM > C
L anterior cerebellum	4.6	−12	−50	−2	467	MAN > NM > C
L SMC (BA 3, 4)	3.9	−30	−28	66	164	MAN > NM = C
D. Manifesting *DYT1* (AV) < controls (AV)[b]						
R DLPFC (BA 9)	4.1	40	10	42	88	MAN = NM < C

a Group differences in rCBF recorded during reaching movements (CCW) are presented in A and B. rCBF differences recorded in the audio-visual reference condition (AV) are presented in C and D. The left most columns reflect local maxima identified in statistical parametric mapping contrasts of only manifesting *DYT1* versus controls. Right-hand columns show the results of the comparisons including non-manifesting *DYT1* in addition to manifesting *DYT1* and controls (see text). Volume-of-interest measurements at the maximum identified in the respective statistical parametric mapping comparisons of manifesting *DYT1* and controls were used for these ANOVAs.
b Comparisons in [CCW–AV] mask of the study population.
c Family-wise error-corrected $P < 0.05$.
d Tukey–Kramer honestly significant difference.
BA = Brodmann area; C = controls; DLPFC =dorsolateral prefrontal cortex; L = left; MAN = manifesting *DYT1*; MNI = Montreal Neurological Institute space; NM = non-manifesting *DYT1*; R = right; SMA = supplementary motor area; SMC = sensorimotor cortex.

non-manifesting *DYT1* and controls for both the AV and CCW conditions ($P<0.05$, Dunett's T3). Notably, normal motor-related activation pattern expression for non-manifesting *DYT1* was within the range of control values for CCW scans (Fig. 3A, left). In contrast, for AV scans (Fig. 3A, right), pattern expression was significantly elevated in non-manifesting *DYT1* carriers relative to controls ($P<0.05$, Dunett's T3).

Normal motor-related activation pattern expression measured in the AV scans correlated ($r=0.70$, $P=0.04$) with concurrent BFMDRS motor ratings (Fig. 3B). These clinical ratings did not correlate significantly with normal motor-related activation pattern expression measured in the CCW scans ($r=0.49$, $P=0.2$). We note that there was no difference between normal motor-related activation pattern values from the group that was used for pattern derivation ($n=18$) and those computed on a prospective case basis in the subsequent control group (controls, $n=12$), whether quantified in AV or CCW scans ($P>0.2$).

Discussion

The results of this study demonstrate that overactivity of the sensorimotor network, as manifested by abnormally increased normal motor-related activation pattern expression in DYT1 carriers, is an important and quantifiable trait feature of DYT1 dystonia (Edwards *et al.*, 2003; Rothwell and Huang, 2003; Quartarone *et al.*, 2006). While these abnormalities were evident at the network level, significant regional changes were also discerned, with increased activation of the sensorimotor cortex as the most salient finding in affected carriers. That said, whether clinically penetrant or not, the gene carriers exhibited elevated activation of auxiliary motor and parietal association regions. These findings indicate that in DYT1 dystonia, increased cortical excitability is not restricted to the sensorimotor cortex and that higher order motor and sensory integration areas may be involved as a trait feature of the disorder. Similar findings have been reported in functional imaging studies of sporadic dystonia (Odergren *et al.*, 1998; Preibisch *et al.*, 2001; Dresel *et al.*, 2006; Tecchio *et al.*, 2008), suggesting mechanistic similarity with hereditary forms of the disorder.

The regional activation observed on univariate as well as multivariate image analysis accord with what is known of the neural mechanisms that mediate self-initiated reaching movements (Winstein *et al.*, 1997; Scott, 2003) with goal-directed orientation (Buneo *et al.*, 2002). In this regard, normal motor-related activation pattern expression in individual subjects can be interpreted as a quantitative descriptor of sensorimotor network activity measured in either the motor (CCW) or non-motor (AV) conditions. Of note, pattern expression in the latter condition was found to correlate with independent clinical severity ratings,

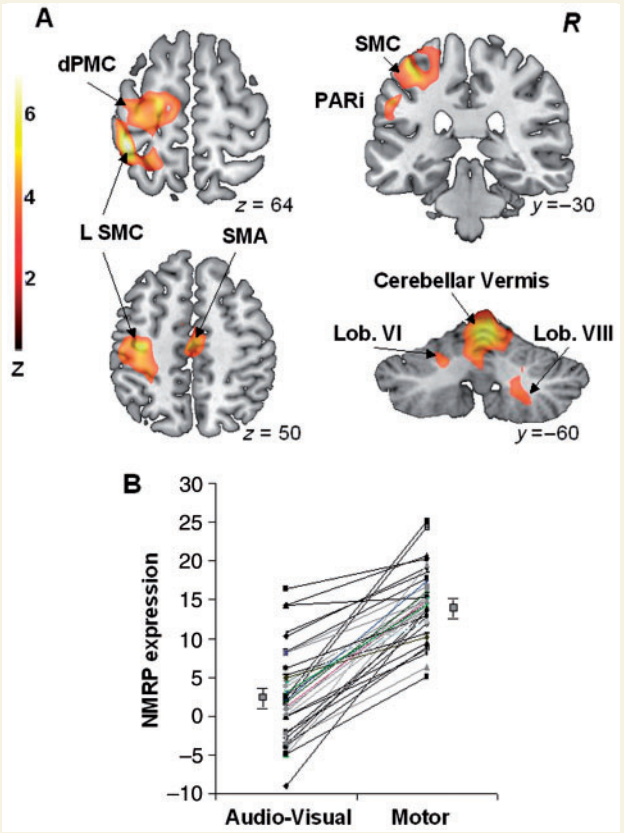

Figure 2 The normal motor-related activation pattern. (**A**) Normal motor-related activation pattern (NMRP) identified by ordinal trends canonical variates analysis (OrT/CVA) of 78 $H_2^{15}O$ PET scans (39 CCW- and 39 AV) acquired in 18 healthy volunteer subjects (see text). This spatial covariance pattern was characterized by activation of the left sensorimotor cortex (SMC), premotor cortex (dPMC) and inferior parietal cortex (Table 3). Additional regional contributions to network activity were found bilaterally in the cerebellar vermis and hemispheres. [The colour scale represents positive voxel weights thresholded at $Z = 3.09$, corresponding to regions that contributed significantly ($P < 0.001$) to network activity and which were also reliable ($P < 0.001$) on bootstrap estimation.] (**B**) Normal motor-related activation pattern expression in the subjects comprising the original derivation sample. For all subjects and runs, the expression of this pattern increased during the performance of the motor task ($P < 0.0001$; see text).

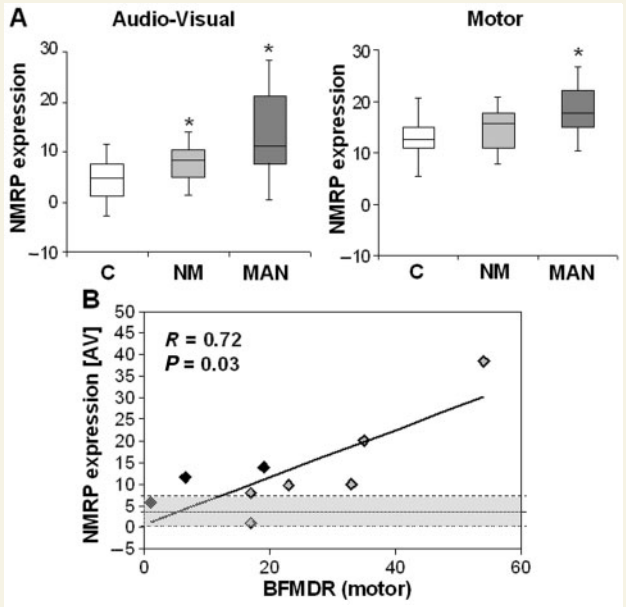

Figure 3 Normal motor-related activation pattern expression in *DYT1* mutation carriers. (**A**) Box-whisker plots of normal motor-related activation pattern expression recorded in the AV reference condition (AV, left) and during movement (right). In the AV condition, pattern expression was elevated in both the manifesting and non-manifesting *DYT1* groups, with the latter positioned between the affected carriers and the controls. In the motor condition, significant increases in normal motor-related activation pattern expression were evident only for the affected carriers. [Significant *post hoc* comparisons with controls ($P < 0.05$) are denoted by asterisks; see text.] (**B**) Normal motor-related activation pattern expression in manifesting *DYT1* carriers measured in the AV condition correlated with clinical severity ratings according to the BFMDRS. (Black diamonds: subjects without contractions at rest; grey diamonds: subjects with constant or with occasional contractions at rest. The normal mean and range are indicated by the shaded area).

suggesting the potential of this network measure as an objective treatment biomarker for use in trials of new therapeutic interventions for this disorder. For instance, the efficacy of pallidal deep brain stimulation is well established in primary generalized dystonia (e.g. Vidailhet *et al.*, 2005; Kupsch *et al.*, 2006). However, there is high inter-individual variability in the time course of clinical response and in overall improvement (Alterman *et al.*, 2007; Isaias *et al.*, 2008). Moreover, functional imaging with $H_2^{15}O$ PET can be advantageous in studies of surgical interventions for dystonia because of the safety concerns involving MRI in patients with implanted deep brain stimulation electrodes. Similar challenges may exist in the assessment of novel interventions for dystonia (e.g. Gonzalez-Alegre *et al.*, 2005; Jinnah and Hess, 2008). Indeed, the development and validation of objective and reliable biomarkers of treatment efficacy is likely to facilitate the evaluation of new therapies (*cf.* Feigin *et al.*, 2007).

We recognize that the observed correlation between normal motor-related activation pattern activity and clinical severity ratings may be a reflection of the presence of dystonic contractions during the scan. This may be particularly relevant in patients with generalized dystonia and high normal motor-related activation pattern expression in 'non-motor' conditions. Nonetheless, abnormal increases in normal motor-related activation pattern activity were also observed in *non-manifesting* carriers scanned in the AV experimental condition. In this circumstance, the scans were free of the potential confound of involuntary movement. Moreover, motor-related activation pattern values from the two subjects with task-specific dystonia (who were demonstrably free of dystonic contractions during scanning in the AV condition) also fell outside the control range (see Fig. 3). The current observations are entirely preliminary; future studies, particularly in subjects with

Table 3 Regions with significant contributions to the normal motor-related activation pattern

Brain region	Coordinates (MNI)			
	Z	*x*	*y*	*z*
Positive loadings[a]				
L sensorimotor cortex (BA 1–4)	7.0	−37	−43	60
L SMC	5.9	−36	−18	50
L dorsal premotor cortex (BA6)	7.6	−22	−16	71
Supplementary motor area (BA 6)	4.9	−2	−17	50
R cingulate cortex (BA 24)	4.3	6	−14	50
L cingulate cortex (BA 31)	3.5	−8	−26	41
L superior parietal (BA 5, BA 7)	4.2	−22	−48	64
L inferior parietal (BA 40)	4.3	−54	−32	34
Occipital association cortex (BA 18, 31)	3.8	−1	−77	14
Vermis	6.9	6	−71	−18
L anterior cerebellar cortex	4.1	−20	−60	−26
R deep cerebellar nuclei	3.2	22	−41	−33
R inferior cerebellar cortex	3.4	22	−60	−44
Negative loadings[a]				
R temporal cortex (BA 21)	3.7	60	−44	−4
R inferior parietal (BA 40)	4.2	60	−54	24
R DLPFC (BA 46)	3.4	48	30	16
R DLPFC (BA 9)	3.7	38	7	46
L DLPFC (BA 9)	3.5	−46	7	46

a Regional contributions to normal motor-related activation pattern activity were considered significant for $Z > 3.09$, $P < 0.001$ (see text).
BA = Brodmann area; DLPFC = dorsolateral prefrontal cortex; L = left; MNI = Montreal Neurological Institute space; R = right; SMC = sensorimotor cortex.

focal dystonia, will be needed to confirm the correlation between normal motor-related activation pattern scores and concurrent clinical dystonia ratings.

The current findings are also consistent with impaired sensory function in DYT1 dystonia. We note that the increase in normal motor-related activation pattern expression was proportionately larger in the AV condition relative to movement (CCW). Indeed, patients with DYT1 dystonia exhibited an almost 4-fold increase in pattern expression relative to controls when measured in the AV condition. In contrast, the normal motor-related activation pattern increase was <2-fold when measured during CCW performance. It has long been debated whether dystonia represents a primarily sensory as opposed to motor disorder (Hallett, 1995; *cf.* Defazio *et al.*, 2007; Tinazzi *et al.*, 2009). In contrast to sporadic focal dystonia, behavioural studies of somatosensory processing in DYT1 carriers have yielded inconsistent findings. Spatial discrimination thresholds have been found to be intact (Molloy *et al.*, 2003), while abnormalities in tactile and visuo-tactile temporal discrimination thresholds have been reported in both manifesting and non-manifesting DYT1 carriers (Fiorio *et al.*, 2007).

Although our results are consistent with previous neurophysiological studies in sporadic as well as DYT1 dystonia, discrepancies with earlier functional imaging studies in sporadic dystonia remain unresolved. Abnormally increased sensorimotor cortex activation has been reported in investigations of focal action-specific dystonia (Odergren *et al.*, 1998; Pujol *et al.*, 2000; Preibisch *et al.*, 2001; Blood *et al.*, 2004; Lerner *et al.*, 2004; Hu *et al.*, 2006) and of secondary dystonia (Ceballos-Baumann *et al.*, 1995*a*; Lehericy *et al.*, 2004). Nonetheless, abnormally decreased sensorimotor cortex activation has also been reported in focal dystonia (Ceballos-Baumann *et al.*, 1995*b*; Ibanez *et al.*, 1999; Oga *et al.*, 2002; Haslinger *et al.*, 2005; Dresel *et al.*, 2006), as well as in idiopathic generalized dystonia (Ceballos-Baumann *et al.*, 1995*a*; Playford *et al.*, 1998). Abnormally increased activation of secondary motor cortices appears to be a consistent finding across the dystonia spectrum (Ceballos-Baumann *et al.*, 1995*a*, *b*; 1997; Odergren *et al.*, 1998; Lehericy *et al.*, 2004; Lerner *et al.*, 2004; Hu *et al.*, 2006), although reports also exist of abnormally reduced activation in these areas (Ibanez *et al.*, 1999; Pujol *et al.*, 2000; Haslinger *et al.*, 2005; Dresel *et al.*, 2006). It is possible that these inconsistencies are attributable to differences in experimental paradigms and analytical strategies. In particular, functional MRI studies inherently rely on the difference in blood oxygen level-dependent signal between states as a measure of activation in brain tissue. As a consequence, these studies may potentially ascribe 'underactivity' to an area with an abnormal increase in baseline neural activity, or 'overactivity' to one with reduced activity at baseline (*cf.* Argyelan *et al.*, 2009).

It is not known whether increased motor cortical excitability and disorganized sensorimotor integration reflect an intrinsic susceptibility to dystonia, or whether these findings represent a consequence of maladaptive reorganization (Rothwell and Huang, 2003). Supporting the former notion, Edwards and colleagues (2003) demonstrated reductions in intra-cortical inhibition in DYT1 carriers irrespective of clinical penetrance. Increased sensorimotor activity in non-manifesting DYT1 carriers, as evident by elevated normal motor-related activation pattern expression in the AV condition, is likewise consistent with an intrinsic abnormality. Notably, this experimental condition did not require tactile

input or motor output. Thus, increases in network activity in this state may be a manifestation of broad changes in higher order multimodal sensory integration. That said, these findings may be specific for the DYT1 genotype. Further studies will be needed to determine their relevance to other forms of primary dystonia.

Lastly, we note that the observed increases of motor cortex activity in DYT1 carriers correlate closely with microstructural changes in the cerebello-thalamic-cortical pathways of the same subjects (Carbon *et al.*, 2008*a*; Argyelan *et al.*, 2009). Indeed, we have found a tight inverse relationship between cerebellar outflow pathway connectivity and concurrently recorded neural activity in the sensorimotor cortex and premotor regions (Argyelan *et al.*, 2009). In contrast, the changes in sensorimotor cortex activity recorded in DYT1 mutation carriers do not correlate with reductions in striatal D_2-receptor binding measured in the same subjects (*cf.* Carbon *et al.*, 2009). Additional multi-modal imaging experiments will be needed to characterize more precisely the relationships between reduced integrity of cerebellar pathways, elevated sensorimotor cortex neural activity and abnormal dopamine neurotransmission in dystonia patients and in non-manifesting carriers of dystonia mutations.

Acknowledgements

We thank Dr Thomas Chaly for valuable radiochemistry support and Mr. Claude Margouleff for technical support. We are also indebted to Mrs Deborah Raymond for participant recruitment.

Funding

The National Institutes of Health (R01 NS 047668 to D.E.), the General Clinical Research Centre of The Feinstein Institute for Medical Research [National Centre for Research Resources, a component of the National Institutes of Health (M01 RR 018535)], and NIH/ NIBIB Grant 5R01EB006204 to C.H.

Supplementary material

Supplementary material is available at *Brain* online.

References

Alterman RL, Miravite J, Weisz D, Shils JL, Bressman SB, Tagliati M. Sixty hertz pallidal deep brain stimulation for primary torsion dystonia. Neurology 2007; 69: 681–8.

Argyelan M, Carbon M, Niethammer M, Ulug AM, Voss HU, Bressman SB, et al. Cerebellothalamocortical connectivity regulates penetrance in dystonia. J Neurosci 2009; 29: 9740–7.

Berardelli A, Rothwell JC, Hallett M, Thompson PD, Manfredi M, Marsden CD. The pathophysiology of primary dystonia. Brain 1998; 121: 1195–212.

Blood AJ, Flaherty AW, Choi JK, Hochberg FH, Greve DN, Bonmassar G, et al. Basal ganglia activity remains elevated after movement in focal hand dystonia. Ann Neurol 2004; 55: 744–8.

Buneo CA, Jarvis MR, Batista AP, Andersen RA. Direct visuomotor transformations for reaching. Nature 2002; 416: 632–6.

Carbon M, Eidelberg D. Abnormal structure-function relationships in hereditary dystonia. Neuroscience 2009; Jan 1 [Epub ahead of print].

Carbon M, Ghilardi MF, Argyelan M, Dhawan V, Bressman SB, Eidelberg D. Increased cerebellar activation during sequence learning in *DYT1* carriers: an equiperformance study. Brain 2008a; 131: 146–54.

Carbon M, Kingsley PB, Tang C, Bressman S, Eidelberg D. Microstructural white matter changes in primary torsion dystonia. Mov Disord 2008b; 23: 234–9.

Carbon M, Niethammer M, Peng S, Raymond D, Dhawan V, Chaly T, et al. Abnormal striatal and thalamic dopamine neurotransmission: Genotype-related features of dystonia. Neurology 2009; 72: 2097–103.

Carbon M, Su S, Dhawan V, Raymond D, Bressman S, Eidelberg D. Regional metabolism in primary torsion dystonia: effects of penetrance and genotype. Neurology 2004a; 62: 1384–90.

Carbon M, Trošt M, Ghilardi MF, Eidelberg D. Abnormal brain networks in primary torsion dystonia. Adv Neurol 2004b; 94: 155–61.

Ceballos-Baumann AO, Passingham RE, Marsden CD, Brooks DJ. Motor reorganization in acquired hemidystonia. Ann Neurol 1995a; 37: 746–57.

Ceballos-Baumann AO, Passingham RE, Warner T, Playford ED, Marsden CD, Brooks DJ. Overactive prefrontal and underactive motor cortical areas in idiopathic dystonia. Ann Neurol 1995b; 37: 363–72.

Ceballos-Baumann AO, Sheean G, Passingham RE, Marsden CD, Brooks DJ. Botulinum toxin does not reverse the cortical dysfunction associated with writer's cramp. A PET study. Brain 1997; 120: 571–82.

de Carvalho Aguiar PM, Ozelius LJ. Classification and genetics of dystonia. Lancet Neurol 2002; 1: 316–25.

Defazio G, Berardelli A, Hallett M. Do primary adult-onset focal dystonias share aetiological factors? Brain 2007; 130: 1183–93.

Dresel C, Haslinger B, Castrop F, Wohlschlaeger AM, Ceballos-Baumann AO. Silent event-related fMRI reveals deficient motor and enhanced somatosensory activation in orofacial dystonia. Brain 2006; 129: 36–46.

Edwards MJ, Huang YZ, Wood NW, Rothwell JC, Bhatia KP. Different patterns of electrophysiological deficits in manifesting and non-manifesting carriers of the *DYT1* gene mutation. Brain 2003; 126: 2074–80.

Efron B, Tibshirani RJ. An introduction to the bootstrap. New York, NY: CRC Press, LLC; 1994.

Eidelberg D, Moeller JR, Antonini A, Kazumata K, Nakamura T, Dhawan V, et al. Functional brain networks in *DYT1* dystonia. Ann Neurol 1998; 44: 303–12.

Feigin A, Kaplitt MG, Tang C, Lin T, Mattis P, Dhawan V, et al. Modulation of metabolic brain networks after subthalamic gene therapy for Parkinson's disease. Proc Natl Acad Sci USA 2007; 104: 19559–64.

Ferrieri RA, Alexoff DL, Schlyer DJ, Wolf AP. Remote processing, delivery and injection of H2[15O] produced from a N2/H2 gas target using a simple and compact apparatus. Appl Radiat Isot 1994; 45: 1149–54.

Fiorio M, Gambarin M, Valente EM, Liberini P, Loi M, Cossu G, et al. Defective temporal processing of sensory stimuli in *DYT1* mutation carriers: a new endophenotype of dystonia? Brain 2007; 130: 134–42.

Genovese CR, Lazar NA, Nichols T. Thresholding of statistical maps in functional neuroimaging using the false discovery rate. Neuroimage 2002; 15: 870–8.

Ghilardi M, Ghez C, Dhawan V, Moeller J, Mentis M, Nakamura T, et al. Patterns of regional brain activation associated with different forms of motor learning. Brain Res 2000; 871: 127–45.

Ghilardi MF, Carbon M, Silvestri G, Dhawan V, Tagliati M, Bressman S, et al. Impaired sequence learning in carriers of the *DYT1* dystonia mutation. Ann Neurol 2003; 54: 102–9.

Gonzalez-Alegre P, Bode N, Davidson BL, Paulson HL. Silencing primary dystonia: lentiviral-mediated RNA interference therapy for *DYT1* dystonia. J Neurosci 2005; 25: 10502–9.

Habeck C, Krakauer JW, Ghez C, Sackeim HA, Eidelberg D, Stern Y, et al. A new approach to spatial covariance modeling of functional

brain imaging data: ordinal trend analysis. Neural Comput 2005; 17: 1602–45.

Hallett M. Is dystonia a sensory disorder? Ann Neurol 1995; 38: 139–40.

Haslinger B, Erhard P, Dresel C, Castrop F, Roettinger M, Ceballos-Baumann AO. ''Silent event-related'' fMRI reveals reduced sensorimotor activation in laryngeal dystonia. Neurology 2005; 65: 1562–9.

Hu XY, Wang L, Liu H, Zhang SZ. Functional magnetic resonance imaging study of writer's cramp. Chin Med J 2006; 119: 1263–71.

Ibanez V, Sadato N, Karp B, Deiber MP, Hallett M. Deficient activation of the motor cortical network in patients with writer's cramp. Neurology 1999; 53: 96–105.

Isaias IU, Alterman RL, Tagliati M. Outcome predictors of pallidal stimulation in patients with primary dystonia: the role of disease duration. Brain 2008; 131: 1895–902.

Jinnah HA, Hess EJ. Experimental therapeutics for dystonia. Neurotherapeutics 2008; 5: 198–209.

Kupsch A, Benecke R, Muller J, Trottenberg T, Schneider GH, Poewe W, et al. Pallidal deep-brain stimulation in primary generalized or segmental dystonia. N Engl J Med 2006; 355: 1978–90.

Lehericy S, Gerardin E, Poline JB, Meunier S, Van de Moortele PF, Le Bihan D, et al. Motor execution and imagination networks in post-stroke dystonia. Neuroreport 2004; 15: 1887–90.

Lerner A, Shill H, Hanakawa T, Bushara K, Goldfine A, Hallett M. Regional cerebral blood flow correlates of the severity of writer's cramp symptoms. Neuroimage 2004; 21: 904–13.

Moeller JR, Habeck C. Reciprocal benefits of mass-univariate and multivariate modeling in brain mapping: applications to event-related functional MRI, H215O and PET. Int J Biomed Imaging 2006; 2006: 1–13.

Molloy FM, Carr TD, Zeuner KE, Dambrosia JM, Hallett M. Abnormalities of spatial discrimination in focal and generalized dystonia. Brain 2003; 126: 2175–82.

Nakamura T, Ghilardi MF, Mentis M, Dhawan V, Fukuda M, Hacking A, et al. Functional networks in motor sequence learning: abnormal topographies in Parkinson's disease. Hum Brain Mapp 2001; 12: 42–60.

Odergren T, Stone-Elander S, Ingvar M. Cerebral and cerebellar activation in correlation to the action-induced dystonia in writer's cramp. Mov Disord 1998; 13: 497–508.

Oga T, Honda M, Toma K, Murase N, Okada T, Hanakawa T, et al. Abnormal cortical mechanisms of voluntary muscle relaxation in patients with writer's cramp: an fMRI study. Brain 2002; 125: 895–903.

Playford ED, Passingham RE, Marsden CD, Brooks DJ. Increased activation of frontal areas during arm movement in idiopathic torsion dystonia. Mov Disord 1998; 13: 309–18.

Preibisch C, Berg D, Hofmann E, Solymosi L, Naumann M. Cerebral activation patterns in patients with writer's cramp: a functional magnetic resonance imaging study. J Neurol 2001; 248: 10–7.

Pujol J, Roset-Llobet J, Rosines-Cubells D, Deus J, Narberhaus B, Valls-Sole J, et al. Brain cortical activation during guitar-induced hand dystonia studied by functional MRI. Neuroimage 2000; 12: 257–67.

Quartarone A, Siebner HR, Rothwell JC. Task-specific hand dystonia: can too much plasticity be bad for you? Trends Neurosci 2006; 29: 192–9.

Rothwell JC, Huang YZ. Systems-level studies of movement disorders in dystonia and Parkinson's disease. Curr Opin Neurobiol 2003; 13: 691–5.

Scott SH. The role of primary motor cortex in goal-directed movements: insights from neurophysiological studies on non-human primates. Curr Opin Neurobiol 2003; 13: 671–7.

Sommer M, Ruge D, Tergau F, Beuche W, Altenmuller E, Paulus W. Intracortical excitability in the hand motor representation in hand dystonia and blepharospasm. Mov Disord 2002; 17: 1017–25.

Tecchio F, Melgari JM, Zappasodi F, Porcaro C, Milazzo D, Cassetta E, et al. Sensorimotor integration in focal task-specific hand dystonia: a magnetoencephalographic assessment. Neuroscience 2008; 154: 563–71.

Tinazzi M, Fiorio M, Fiaschi A, Rothwell JC, Bhatia KP. Sensory functions in dystonia: Insights from behavioral studies. Mov Disord 2009; 24: 1427–36.

Trošt M, Carbon M, Edwards C, Ma Y, Raymond D, Mentis MJ, et al. Primary dystonia: is abnormal functional brain architecture linked to genotype? Ann Neurol 2002; 52: 853–6.

Vidailhet M, Vercueil L, Houeto JL, Krystkowiak P, Benabid AL, Cornu P, et al. Bilateral deep-brain stimulation of the globus pallidus in primary generalized dystonia. N Engl J Med 2005; 352: 459–67.

Walsh R, O'Dwyer JP, Sheikh IH, O'Riordan S, Lynch T, Hutchinson M. Sporadic adult onset dystonia: sensory abnormalities as an endophenotype in unaffected relatives. J Neurol Neurosurg Psychiatry 2007; 78: 980–3.

Winstein CJ, Grafton ST, Pohl PS. Motor task difficulty and brain activity: investigation of goal-directed reciprocal aiming using positron emission tomography. J Neurophysiol 1997; 77: 1581–94.